



ACADEMIC
PRESS

Available online at www.sciencedirect.com

SCIENCE @ DIRECT®

JOURNAL OF
SOLID STATE
CHEMISTRY

Journal of Solid State Chemistry 172 (2003) 127–131

<http://elsevier.com/locate/jssc>

Synthesis and characterization of $\text{La}_4\text{MnCu}_6\text{S}_{10}$

Ismail Ijjaali, Adam D. McFarland, Christy L. Haynes, Richard P. Van Duyne,
and James A. Ibers*

Department of Chemistry, Northwestern University, 2145 Sheridan Road, Evanston, IL 60208-3113, USA

Received 12 August 2002; received in revised form 6 November 2002; accepted 17 November 2002

Abstract

The new quaternary sulfide $\text{La}_4\text{MnCu}_6\text{S}_{10}$ has been synthesized by the reaction of La_2S_3 , MnS , and CuS_2 at 1223 K. This compound crystallizes in a new structure type in space group $P\bar{1}$ of the triclinic system with one formula unit in a cell of dimensions at 153 K of $a = 6.6076(3) \text{ \AA}$, $b = 7.3247(3) \text{ \AA}$, $c = 8.7844(4) \text{ \AA}$, $\alpha = 83.457(1)^\circ$, $\beta = 74.398(1)^\circ$, $\gamma = 89.996(1)^\circ$, and $V = 406.61(3) \text{ \AA}^3$. The structure of $\text{La}_4\text{MnCu}_6\text{S}_{10}$ consists of a three-dimensional framework of interconnected LaS_7 monocapped trigonal prisms, MnS_6 octahedra, and CuS_4 tetrahedra. Band gaps of 2.49 eV in the [100] direction and 2.53 eV in the [001] direction have been derived from optical absorption measurements on a $\text{La}_4\text{MnCu}_6\text{S}_{10}$ single crystal.

© 2003 Elsevier Science (USA). All rights reserved.

Keywords: Lanthanum manganese copper sulfide; Band gap in quaternary sulfide; Synthesis and X-ray structure

1. Introduction

Ternary and quaternary chalcogenides containing a combination of *d*- and *f*-elements are of great interest in solid-state chemistry and materials science because of their physical properties and their rich structural chemistry. A recent review of such compounds is available [1].

Quaternary phases containing an alkali metal or copper, in addition to the chalcogen and the 3*d* and 4*f* metals, are generally conveniently prepared by the reactive flux technique [2]. These compounds usually comprise four elements with different coordination preferences [3] and thus are almost always free of crystallographic disorder. Cu is invariably in the 1+ oxidation state in chalcogenides and is usually tetrahedrally coordinated. Such a tetrahedral coordination is also common for Mn. Nevertheless we decided to investigate the Cu/Mn/La/S system. Here we report the synthesis and band gaps of the new quaternary sulfide $\text{La}_4\text{MnCu}_6\text{S}_{10}$, which crystallizes in a new structural type with octahedrally coordinated Mn^{2+} and hence is free of disorder.

2. Experimental

2.1. Synthesis

Single crystals of $\text{La}_4\text{MnCu}_6\text{S}_{10}$ were obtained from the reaction of La_2S_3 (2.0 mmol, Strem, 97%), Cu_2S (3.0 mmol, Strem, 99.5%), and MnS (2.0 mmol, Strem, 99.9%) in a carbon-coated fused-silica tube with KBr (4 mmol, Aldrich, 99.99%) added to promote crystal growth. The materials were mixed and sealed in the tube that was then evacuated to 5×10^{-5} Torr. The reaction mixture was heated gradually to 1273 K, kept at 1273 K for 5 days, cooled at 0.05 K/min to 973 K, and then the furnace was turned off. The reaction mixture was washed free of bromide salts with water and then dried with acetone. Only a few crystals were obtained. Attempts to prepare this phase in high yield were unsuccessful. Yellow–green, block-shaped crystals of $\text{La}_4\text{MnCu}_6\text{S}_{10}$ were isolated and manually extracted from the melt. The presence of all four elements in an approximate ratio of 4:1:6:10 was confirmed with EDX equipped Hitachi 3500N scanning electron microscope. The compound is stable in air.

2.2. Crystallography

Single-crystal X-ray diffraction data were obtained with the use of graphite-monochromatized $\text{MoK}\alpha$

*Corresponding author. Fax: +1-847-491-2976.

E-mail address: ibers@chem.northwestern.edu (J.A. Ibers).

radiation ($\lambda = 0.71073 \text{ \AA}$) at 153 K on a Bruker Smart-1000 CCD diffractometer [4]. The crystal-to-detector distance was 5.023 cm. Crystal decay was monitored by recollecting 50 initial frames at the end of data collection. Data were collected by a scan of 0.3° in ω in groups of 606, 606, 606, and 606 frames at π settings of 0° , 90° , 180° , and 270° . The exposure time was 15 s/frame. The collection of intensity data was carried out with the program SMART [4]. Cell refinement and data reduction were carried out with the use of the program SAINT [4], and a face-indexed absorption correction was performed numerically with the use of the program XPREP [5]. The program SADABS [4] was then employed to make incident beam and decay corrections.

The structure was solved in the triclinic space group $P\bar{1}$ with the direct methods program SHELXS of the SHELXTL suite of programs [5] and refined by full-matrix least-squares techniques. Final refinements included anisotropic displacement parameters and a secondary extinction correction. The program ADDSYM of the PLATON suite of programs [6] did not suggest any symmetry elements other than the center of inversion. The program STRUCTURE TIDY [7] was used to standardize the positional parameters. Additional experimental details are given in Table 1. Fractional coordinates and equivalent atomic displacement parameters are listed in Table 2, and Table 3 presents selected metrical data.

2.3. Optical measurements

Optical absorption measurements on a $\text{La}_4\text{MnCu}_6\text{S}_{10}$ single crystal, as verified by X-ray diffraction measure-

Table 1
Crystal data and structure refinement for $\text{La}_4\text{MnCu}_6\text{S}_{10}$

Formula weight	1312.42
Space group	$P\bar{1}$
a (Å)	6.6076(3)
b (Å)	7.3247(3)
c (Å)	8.7844(4)
α (°)	83.457(1)
β (°)	74.398(1)
γ (°)	89.996(1)
V (Å ³)	406.61(3)
Z	1
T (K)	153(2)
λ (MoK α)	0.71073
ρ_c (g/cm ³)	5.360
Crystal dimensions (mm)	0.098 × 0.088 × 0.034
μ (cm ⁻¹)	199.3
Transmission factors	0.195–0.521
$R(F)^a$	0.0226
$R_w(F_o^2)^b$	0.0584

^a $R(F) = \sum \|F_o\| - |F_c| / \sum \|F_o\|$ for $F_o^2 > 2\sigma(F_o^2)$.

^b $R_w(F_o^2) = [\sum w(F_o^2 - F_c^2)^2 / \sum wF_o^4]^{1/2}$, $w^{-1} = \sigma^2(F_o^2) + (0.033 \times F_o^2)^2$ for $F_o^2 \geq 0$; $w^{-1} = \sigma^2(F_o^2)$ for $F_o^2 < 0$.

Table 2
Atomic coordinates and equivalent isotropic displacement parameters for $\text{La}_4\text{MnCu}_6\text{S}_{10}$

Atom	x	y	z	$U_{eq}(\text{Å}^2)^a$
La(1)	0.06091(4)	0.40980(3)	0.24570(3)	0.00619(10)
La(2)	0.27739(4)	0.07356(3)	0.82589(3)	0.00645(10)
Mn	$\frac{1}{2}$	$\frac{1}{2}$	$\frac{1}{2}$	0.0112(2)
Cu(1)	0.21784(9)	0.80040(8)	0.33932(8)	0.01291(15)
Cu(2)	0.33467(9)	0.09936(8)	0.42608(7)	0.01172(14)
Cu(3)	0.56175(9)	0.33776(8)	0.05495(7)	0.01100(14)
S(1)	0.08386(17)	0.73082(15)	0.00238(13)	0.0068(2)
S(2)	0.13305(17)	0.30104(15)	0.57327(13)	0.0070(2)
S(3)	0.31796(17)	0.09146(15)	0.16562(13)	0.0073(2)
S(4)	0.47195(17)	0.58655(15)	0.21615(13)	0.0071(2)
S(5)	0.68781(17)	0.19026(15)	0.41663(13)	0.0078(2)

^a U_{eq} is defined as one third of the trace of the orthogonalized U_{ij} tensor.

Table 3
Selected interatomic distances (Å) and angles (deg) for $\text{La}_4\text{MnCu}_6\text{S}_{10}$

La(1)–S(2)	2.886(1)	La(2)–S(1)	2.896(1)
La(1)–S(1)	2.891(1)	La(2)–S(4)	2.922(1)
La(1)–S(5)	2.894(1)	La(2)–S(1)	2.930(1)
La(1)–S(3)	2.924(1)	La(2)–S(3)	2.950(1)
La(1)–S(4)	2.944(1)	La(2)–S(2)	2.984(1)
La(1)–S(1)	2.967(1)	La(2)–S(5)	3.000(1)
La(1)–S(2)	3.059(1)	La(2)–S(3)	3.085(1)
Cu(1)–S(2)	2.330(1)	Cu(3)–S(1)	2.327(1)
Cu(1)–S(5)	2.396(1)	Cu(3)–S(3)	2.357(1)
Cu(1)–S(4)	2.419(1)	Cu(3)–S(4)	2.411(1)
Cu(1)–S(3)	2.455(1)	Cu(3)–S(4)	2.452(1)
Cu(1)–Cu(2)	2.582(1)	Cu(3)–Cu(3)	2.674(1)
Cu(2)–S(2)	2.267(1)	Mn–S(4) × 2	2.558(1)
Cu(2)–S(3)	2.327(1)	Mn–S(5) × 2	2.667(1)
Cu(2)–S(5)	2.378(1)	Mn–S(2) × 2	2.714(1)
Cu(2)–S(5)	2.404(1)		
S(2)–Cu(1)–S(5)	102.76(5)	S(1)–Cu(3)–S(3)	116.87(5)
S(2)–Cu(1)–S(4)	117.28(5)	S(1)–Cu(3)–S(4)	113.44(4)
S(5)–Cu(1)–S(4)	99.78(4)	S(3)–Cu(3)–S(4)	108.61(4)
S(2)–Cu(1)–S(3)	120.30(5)	S(1)–Cu(3)–S(4)	99.74(4)
S(5)–Cu(1)–S(3)	110.69(4)	S(3)–Cu(3)–S(4)	104.35(4)
S(4)–Cu(1)–S(3)	104.13(4)	S(4)–Cu(3)–S(4)	113.31(4)
S(2)–Cu(2)–S(3)	118.40(5)	S(4)–Mn–S(4)	180
S(2)–Cu(2)–S(5)	109.24(5)	S(5)–Mn–S(2)	86.25(3)
S(3)–Cu(2)–S(5)	116.02(5)	S(4)–Mn–S(5)	89.61(3)
S(2)–Cu(2)–S(5)	103.88(5)	S(4)–Mn–S(2)	89.79(3)
S(3)–Cu(2)–S(5)	107.83(4)		
S(5)–Cu(2)–S(5)	98.84(4)		

ments, were performed with the use of an Ocean Optics model S2000 spectrometer over the range 400 nm (3.10 eV) to 800 nm (1.55 eV) at 293 K. The resolution of the spectrometer is approximately 1 nm (0.01 eV resolution at 2.5 eV). The spectrometer was coupled by fiber optics to a Nikon TE300 inverted microscope. White light originated from the TE300 lamp and passed through a polarizer before reaching the sample. The crystal, aligned along its b axis, was positioned at the focal point above the $20\times$ objective by means of a goniometer mounted on translation stages (Line Tool

Company). The light transmitted through the crystal was then spatially filtered before being focused into the 400 μm core diameter fiber coupled to the spectrometer. Fine alignment of the microscope assembly was achieved by maximizing the transmission of the lamp profile. The excitation white light was polarized perpendicular to the crystal a axis. The optical band gap was calculated from the absorption spectrum by means of a simple inflection point analysis that does not require a correction for crystal thickness or a spot size fill factor and is independent of the spectral baseline.

3. Results and discussion

$\text{La}_4\text{MnCu}_6\text{S}_{10}$ crystallizes in new structure type. The unique metal-atom environments and labeling scheme are shown in Fig. 1. The crystallographic asymmetric unit contains two La atoms, one Mn atom, three Cu atoms, and five S atoms. The Mn atom sits at a center of inversion. The two independent La atoms are each coordinated by S atoms in a monocapped trigonal prism; each of the three independent Cu atoms is tetrahedrally coordinated by S atoms; the Mn atom is surrounded by six S atoms in a slightly distorted octahedron. There is no disorder. There is no S–S

bonding in $\text{La}_4\text{MnCu}_6\text{S}_{10}$, the shortest S–S distance being 3.548(2) Å. Hence formal oxidation states 3+, 2+, 1+, and 2–, respectively, may be assigned to La, Mn, Cu, and S in this compound.

As shown in Fig. 2, two $\text{La}(1)\text{S}_7$ monocapped trigonal prisms share two edges (S1–S1 and S2–S2) and two $\text{La}(2)\text{S}_7$ monocapped trigonal prisms also share two edges (S1–S1 and S3–S3). The connection between the $\text{La}(1)\text{S}_7$ and $\text{La}(2)\text{S}_7$ prisms is made by the sharing of four vertices and three edges. The La–S distances range from 2.886(1) to 3.085(1) Å and are comparable with La–S distances in LaCuS_2 of 2.891(4) to 3.081(4) Å [8].

Each $\text{Cu}(2)\text{S}_4$ tetrahedron has one edge-sharing neighbor along a and each $\text{Cu}(3)\text{S}_4$ tetrahedron has one edge-sharing neighbor along b to form $[\text{Cu}_2\text{S}_5]$ bitetrahedra that link to each other by the sharing of S3 corners along c (Fig. 3). In addition, each $\text{Cu}(1)\text{S}_4$ tetrahedron completes this three-dimensional connection by sharing corners and edges with $\text{Cu}(2)\text{S}_4$ tetrahedra, and only corners with $\text{Cu}(3)\text{S}_4$ tetrahedra. These CuS_4 tetrahedra are significantly distorted, with S–Cu–S angles in the range 98.84(4)–120.30(5)°. The Cu–S bond lengths are in the range 2.267(1)–2.455(1) Å, compared with 2.337(5)–2.537(5) Å in LaCuS_2 (8) and 2.372(1)–2.398(1) Å in BaLaCuS_3 [9]. The Cu–Cu distances of 2.583(1) and 2.674(1) Å may be compared with those of 2.749(1) Å in LaCuS_2 [10], 2.644(6) Å in LaCuS_2 (8), and 2.557(1) Å in Cu [11].

Each MnS_6 octahedron, which has a crystallographically imposed inversion center, shares four edges with $\text{La}(1)\text{S}_7$, as well as two edges and two corners with $\text{La}(2)\text{S}_7$ prisms (Fig. 3). Additionally, this octahedron connects through apex- and edge-sharing to $\text{Cu}(1)\text{S}_4$ and $\text{Cu}(2)\text{S}_4$ tetrahedra, and only by apex-sharing to $\text{Cu}(3)\text{S}_4$ tetrahedra. The MnS_6 octahedron is only slightly distorted, with angles of 86.25(3)°, 89.61(3)°, and 89.79(3)°. The Mn–S distances range from 2.558(1) to 2.714(1) Å. These distances are comparable with those found in those few reported $\text{Ln}/\text{Mn}/\text{S}$ compounds in which Mn adopts octahedral coordination, namely $\text{La}_6\text{MnSi}_2\text{S}_{14}$ (2.637–2.674 Å) [12], $\text{La}_3\text{MnFeS}_7$ (2.773–2.816 Å) [13], and $\text{La}_6\text{Mn}_2\text{Ga}_2\text{S}_{14}$ (2.581–2.622 Å) [14].

The optical absorption spectrum and its second derivative of absorbance versus photon energy are displayed in Fig. 4 for light impinging on the (100) crystal face of a $\text{La}_4\text{MnCu}_6\text{S}_{10}$ single crystal. Analysis leads to a band gap of 2.49 eV. Similar analysis of the absorption spectrum for light impinging on the (001) face leads to a band gap of 2.53 eV. Given the resolution of the spectrometer, the difference of 0.04 eV in these band gaps is probably significant. Less significant variations with direction have been observed in the three-dimensional phase $\text{La}_3\text{CuO}_2\text{S}_3$ [15], whereas larger variations are found in the layered CsLnZnSe_3 compounds [16].

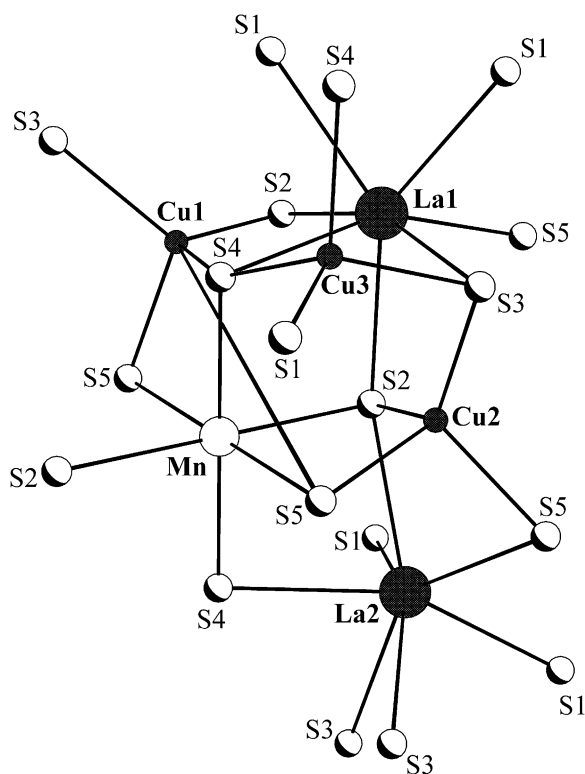


Fig. 1. Metal-atom environments in the structure of $\text{La}_4\text{MnCu}_6\text{S}_{10}$.

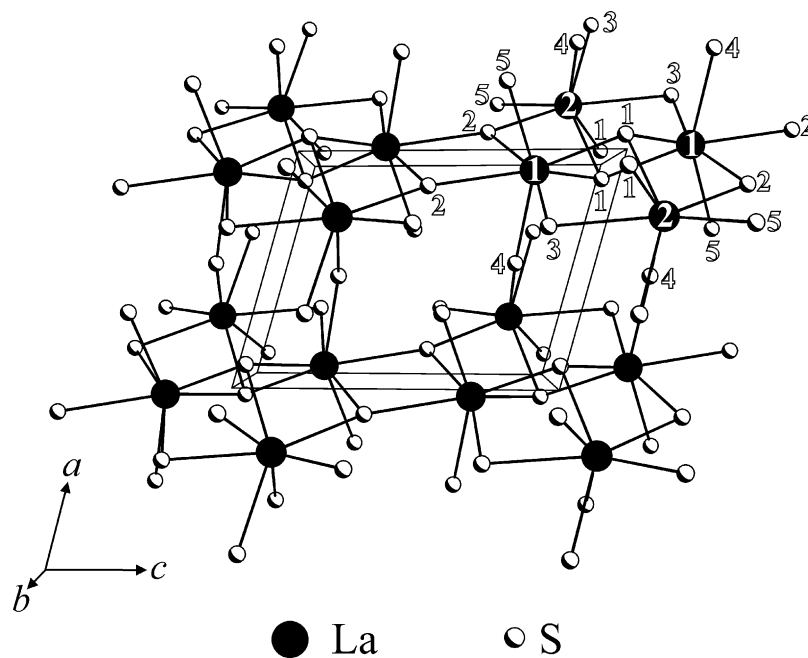


Fig. 2. The La/S fragment of $\text{La}_4\text{MnCu}_6\text{S}_{10}$ viewed down [010].

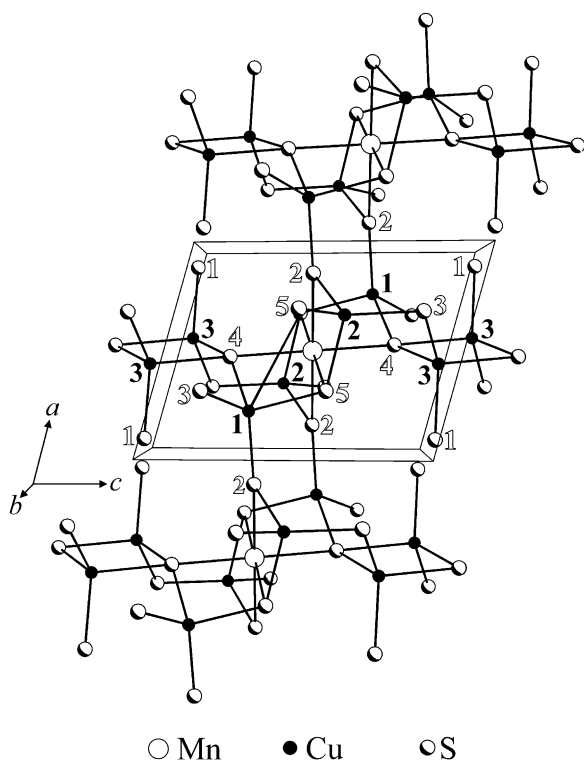


Fig. 3. CuS_4 tetrahedra and MnS_6 octahedra linkage in $\text{La}_4\text{MnCu}_6\text{S}_{10}$ as viewed along [010].

Acknowledgments

This research was supported by NSF Grant No. DMR00-96676 (JAI) and a GlaxoSmithKline-sponsored ACS Division of Analytical Chemistry fellowship to CLH. Use was made of the MRL Central Facilities

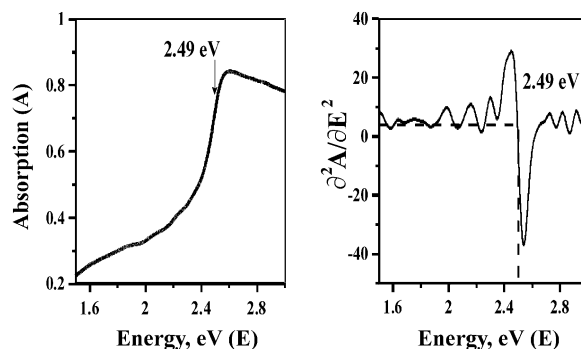


Fig. 4. Optical absorption spectrum (left) and band gap calculation (right) for $\text{La}_4\text{MnCu}_6\text{S}_{10}$. The light impinges on the (100) crystal face.

supported by the National Science Foundation at the Materials Research Center of Northwestern University under Grant No. DMR00-76097.

References

- [1] K. Mitchell, J.A. Ibers, *Chem. Rev.* 102 (2002) 1929–1952.
- [2] S.A. Sunshine, D. Kang, J.A. Ibers, *J. Am. Chem. Soc.* 109 (1987) 6202–6204.
- [3] S.A. Sunshine, D.A. Keszler, J.A. Ibers, *Acc. Chem. Res.* 20 (1987) 395–400.
- [4] Bruker, SMART Version 5.054 Data Collection and SAINT-Plus Version 6.22 Data Processing Software for the SMART System, Bruker Analytical X-ray Instruments, Inc., Madison, WI, USA, 2000.
- [5] G.M. Sheldrick, SHELXTL DOS/Windows/NT Version 6.12, Bruker Analytical X-ray Instruments, Inc., Madison, WI, USA, 2000.

- [6] A.L. Spek, *Acta Crystallogr. A: Found. Crystallogr.* 46 (1990) C34.
- [7] L.M. Gelato, E. Parthé, *J. Appl. Crystallogr.* 20 (1987) 139–143.
- [8] M. Julien-Pouzol, S. Jaulmes, A. Mazurier, M. Guittard, *Acta Crystallogr. B: Struct. Crystallogr. Cryst. Chem.* 37 (1981) 1901–1903.
- [9] A.E. Christuk, P. Wu, J.A. Ibers, *J. Solid State Chem.* 110 (1994) 330–336.
- [10] F.Q. Huang, J.A. Ibers, *Inorg. Chem.* 38 (1999) 5978–5983.
- [11] M.E. Straumanis, L.S. Yu, *Acta Crystallogr. A: Cryst. Phys. Diffr. Theor. Gen. Crystallogr.* 25 (1969) 676–682.
- [12] G. Collin, P. Laruelle, *C.R. Seances Acad. Sci. Ser. C* 270 (1970) 410–412.
- [13] K.S. Nanjundaswamy, J. Gopalakrishnan, *J. Solid State Chem.* 49 (1983) 51–58.
- [14] N. Rodier, M. Guittard, J. Flahaut, *C. R. Acad. Sci. Sér 2* 296 (1983) 65–70.
- [15] I. Ijjaali, C.L. Haynes, A.D. McFarland, R.P. Van Duyne, J.A. Ibers, *J. Solid State Chem.* (2003), in press.
- [16] K. Mitchell, C.L. Haynes, A.D. McFarland, R.P. Van Duyne, J.A. Ibers, *Inorg. Chem.* 41 (2002) 1199–1204.